Effect of Fibrillar Morphology on Elastomer-Modified Polypropylene

ZHANG LING, HUANG RUI, LI LIANGBIN, WANG GANG

Department of Polymer Materials Science and Engineering, Sichuan University, Chengdu, Sichuan 610065, China

ABSTRACT: Blends of polypropylene (PP) with a copolymer of ethylene and octene (EOC) were studied. The effect of viscosity ratio of elastomer domains to the matrix PP η_d/η_m (where subscript d and m designate dispersed phase and matrix, respectively) on fibril formation was investigated. Fibril morphology was observed for both $\eta_d/\eta_m \approx 1$ and $\eta_d/\eta_m > 1$ ($\eta_d/\eta_m = 1.70$ or 2.40). As the viscosity ratio increased further, the spherical, elliptical, and rodlike morphology appeared. Fibril formation at $\eta_d/\eta_m > 1$ is possibly attributed to the effect of the interface interaction between the two phases. With soft fibril formation of EOC in PP, mechanical properties of the blends such as tensile and flexural properties were not improved and the impact strength was low compared to those of blends with spherical, elliptical, and rodlike dispersed morphology. © 2002 John Wiley & Sons, Inc. J Appl Polym Sci 83: 1870–1874, 2002

Key words: polypropylene; ethylene–octene copolymer; soft fibril; viscosity ratio

INTRODUCTION

Toughness is a very important property for many applications of materials that greatly depend on the morphology. A profound understanding of the relationship between the morphology and properties of polymers is important for the development of polymer systems with improved toughness. In recent years, use of elastomers as the impact modifiers of polymers is well documented in the literature. Blends of polypropylene (PP) with various impact modifiers have been investigated in the literature, such as ethylene–propylene rubber (EPR),[1] ethylene–propylene–diene rubber (EPDM),[2] ethylene–hexene rubber,[3] styrene–ethylene butylene–styrene rubber (SEBS),[4,5] and so forth. A recent addition to the family of thermoplastic elastomers is ethylene–octene copolymer (EOC), which is catalyzed by homogeneous metallocene catalysts.

In immiscible polymer blends, the properties greatly depend on the morphology, which is basically determined by the following factors: (1) processing conditions, (2) blend composition, (3) interface interaction, and (4) the viscosity ratio of components.[6] In spite of many studies on this subject, the effect of viscosity ratio on fibril formation remains of particular interest. As early as 1934, Taylor showed that the deformation of drops in a liquid substantially depends on the viscosities of the phases involved.[7] There has been some discussion about fibril formation based on the viscosity ratio of the base materials.[8,9] With regard to the viscosity effect on PP/rubber blends, rubber generally disperses in the shape of spherulite in PP matrix as a result of the higher viscosity of rubber than that of PP.[10–14] However, the effect of the viscosity ratio on fibril formation in the PP/elastomer system is rarely studied.[15,16]

In this investigation we chose ethylene–octene copolymer (EOC) as an impact modifier for PP. The state of dispersion of EOC domains to PP is explored by changing the viscosity ratio. Fibrillar

Table I Physical Properties of Base Polymers

Material[a]	Density (g/cm^3)	MFI (g/10 min)	1-Octene Content (wt %)	Producer
PP1	0.90	1.1	—	1300, Yanshan Chemical
PP2	0.91	13	—	S700, Yangzi Chemical
EOC1	0.87	5	24	8200, Dupont–Dow Chemical
EOC2	0.863	0.5	28	8180, Dupont–Dow Chemical

[a] PP: MFI under 2.16 kg load at 230°C; EOC: MFI under 2.16 kg load at 190°C.

morphology was observed in the case of both $\eta_d/\eta_m \approx 1$ and $\eta_d/\eta_m > 1$. The aim of this work was to examine the principles of soft fibril formation and to establish morphology–property relationships of PP/EOC binary blends.

EXPERIMENTAL

Materials and Blend Preparation

The two types of PP and two types of EOC used in the present experiments are listed in Table I. Blends were prepared by melt mixing in a corotating twin-screw extruder (D = 25 mm, L/D = 32; TSSJ-25/32, China) at a components ratio of 75/25. The extrusion process was performed at 120 rpm in the 190–200°C temperature range. The basic formulations of these blends are listed in Table II.

Measurements

Rheological properties of the base materials were measured using a capillary rheometer (D5052M; Kayeness, Inc.) with L/D of 40 at 190°C.

Specimens for tensile, flexural, and Izod impact testing were prepared by an injection-molding machine (PS40E5ASE; Nissei) at an injection temperature of 200°C. Tensile (GB1040), flexural (GB9341), and impact (GB1843) properties of injection-molded samples were investigated using a tensile tester (AG-10TA; Shimadzu Corp., Japan)

and Izod impact tester (XJU-2.75; China) at 23°C. At least five runs were made and the results were averaged.

The dispersed morphology of the blends was determined by a scanning electron microscope (X-650; Hitachi, Tokyo, Japan). Injection-molded tensile specimens were cryogenically fractured in liquid nitrogen along the flow direction (L direction) and perpendicular to the flow direction (T direction) in the mold. The fractured surfaces were etched in n-heptane for 5 min at 50°C and sputtered with gold before viewing.

SEM was also used to study the morphology of cavitation of the Izod samples. The broken Izod samples were cryofractured along planes perpendicular to the fracture surfaces. The exposed surfaces were then coated with gold and examined under SEM.

RESULTS AND DISCUSSION

Rheology

The apparent viscosities of the base materials are shown in Figure 1. The viscosity of EOC2 is by far the highest and PP2 has the lowest throughout the shear rate range tested. At low shear rate, the viscosity of EOC1 is lower than that of PP1; however, it is higher at high shear rate, resulting in a viscosity crossover at approximately $r' = 800$ s^{-1}.

Morphology

Figures 2 and 3 show the SEM micrographs of the dispersed morphology of the blends. In transverse direction to flow (Fig. 2), EOC particles are uniformly dispersed (0.3–0.5 μm) in the PP matrix. The dispersed domains become larger with the increase of viscosity ratio (comparing a and b with A and B, respectively).

Table II Formulation of the Blends

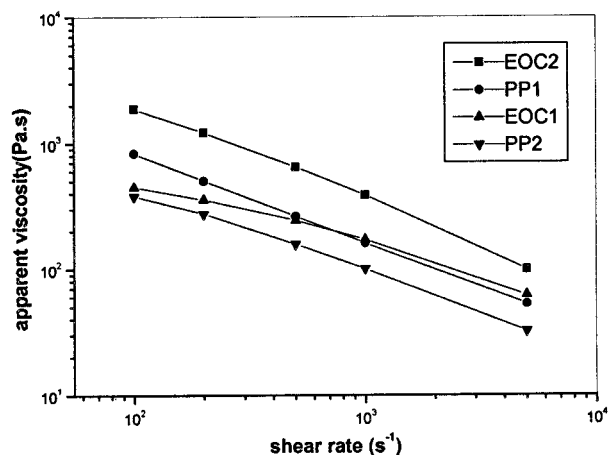| Run	PP1	PP2	EOC1	EOC2
a	75	—	25	—
b	75	—	—	25
A	—	75	25	—
B	—	75	—	25

Figure 1 The apparent viscosities of the base materials.

Drop-to-fibril transition in Newtonian fluids was previously studied by various investigators.[7,17,18] They point out that the major parameter for fibril formation was the viscosity ratio. They reported that if the viscosity ratio was close
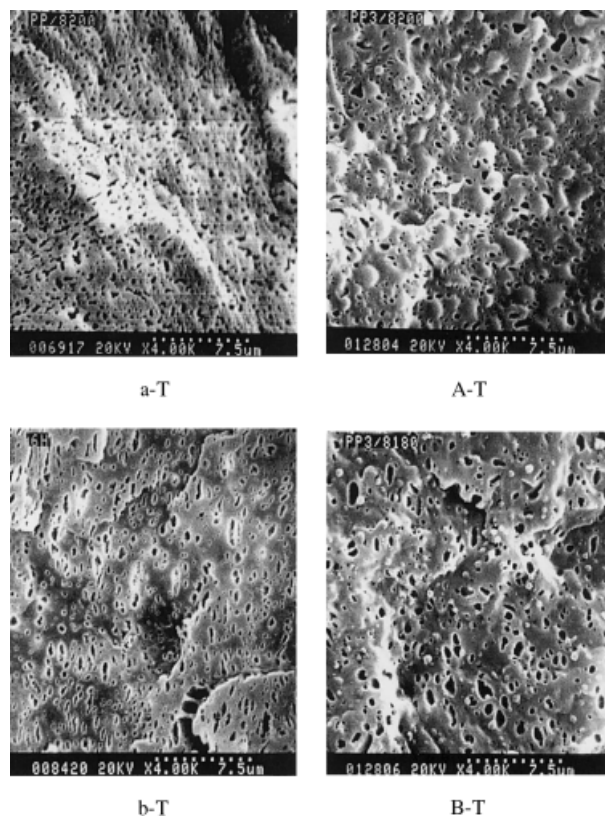

Figure 2 SEM micrographs of the blends (transverse direction): a-T, A-T, b-T, B-T.
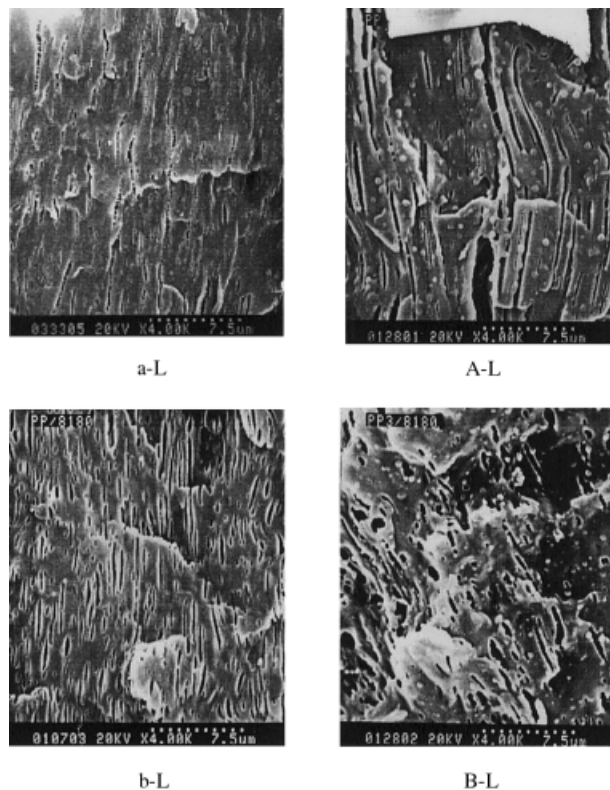

Figure 3 SEM micrographs of the blends (longitudinal direction): a-L, A-L, b-L, B-L.

to unity, a uniform thin-thread fibril was formed. The viscosity ratio, recalculated for the appropriate shear rate (10^3 s^{-1}) at 190°C, and the longitudinal morphologies of the blends are summarized in Table III. It is interesting to find that fibrils are formed along the flow direction (Fig. 3) regardless of the viscosity ratio of EOC to PP. Run a corresponds to $\eta_d/\eta_m \approx 1$, and runs A and b, to $\eta_d/\eta_m > 1$. However, elongated fibrils are observed in three cases. For the PP/rubber system, fibril formation was reported at $\eta_d/\eta_m < 1$,[15] which considered the influence of the viscosity ratio only. In fact, the morphology of dispersion is influenced by many factors.[6] The deformability of

Table III Viscosity Ratio and Longitudinal Phase Morphology of the Blends

Run	Fibrillation (L Direction)	η_d/η_m
a	Fine long fibril	1.06
b	Coarse short fibril	2.40
A	Coarse long fibril	1.70
B	Irregular shapes	3.84

the drop formed by a Newtonian liquid[17] is determined by two parameters: (1) the ratio (λ) of the viscosity of the dispersed phase to the viscosity of the continuous phase and (2) the ratio (K) of the interfacial tension (λ) to the product of the shear stress (τ) and the radius of the particle a:

$$\lambda = \frac{\eta_d}{\eta_m} \qquad (1)$$

$$K = \frac{\gamma}{\tau a} \qquad (2)$$

The numerator of eq. (2) is the resistant force against the deformation and the denominator is the driving force for the dispersed-phase deformation; then deformation occurs only for K lower than a critical value. Typical shear stress values ($\tau = \eta_m r'$) in polymer blends are 10^4 to 10^5 Pa and $\gamma = 5 \times 10^{-3}$ N/m. Thus, for drops larger than a micron, the value $K \ll 1.0$, and the deformation becomes a function of the viscosity ratio of the melts only. For submicron drops, the value of $K \gg 1.0$, which means that interface interaction will play a great role in the deformation.

In our experiment the composition of the blends and the processing conditions were constant, and the size of the dispersed domains was at 0.3 to 0.5 μm. Therefore, the fibril arising in runs A and b is probably ascribed to the effect of the interfacial interaction between the two phases. High interfacial tension will generally lead to discrete phases. Carriere and Silvis[19] studied the interfacial tension of polypropylene/ethylene–octene copolymer with different octene content and revealed that the interfacial tension decreased monotonically with increasing octene content, resulting in improved compatibility, which implied lower interfacial tension and better compatibility between PP and EOC2 than between PP and EOC1 in our case. The problem is that there is a lack of reliable experimental data for evaluating the interfacial tension (γ). In Figure 2 (panel B-L), the minor component dispersed more coarsely in spherical, elliptical, and short rodlike domains because, when the viscosity of the minor component is significantly higher than that of the major component, the dispersed phase experiences less deformation than that imposed on the continuous phase and is easy to accumulate.

Table IV   Mechanical Properties of the Blends and the Matrices

Run	Tensile Strength (MPa)	Flexural Strength (MPa)	Flexural Modulus (MPa)	Impact Strength (kJ/m^2)
a	25.0	28.7	869.2	43.9
A	21.2	28.9	976.4	13.4
b	24.0	28.8	863.0	47.5
B	21.0	31.6	993.1	39.6
PP1	33.2	43.3	1301.6	4.8
PP2	28.2	46.4	1461.1	2.6

Mechanical Properties

Tensile and Flexural Properties

Mechanical properties of the blends are listed in Table IV. The tensile and flexural properties of PP are decreased with the addition of elastomer. The decrease in both strength and modulus is a slightly greater than the rule of mixture expected for a blend with well-dispersed particles. To our surprise, unlike rigid fibers such as glass fiber and LCP *in situ* fiber, which can reinforce the matrix, such soft fibril seems to have no effect on tensile and flexural properties. This may be attributed to very low strength and modulus of EOC, which contributes little to load sharing.

Izod Impact Properties

Incorporation of elastomer in PP resulted in a significant improvement in the impact strength of the binary blends, which is the response of morphology. In toughened PP, the rubber particles have a dual role: (1) they act as stress concentrators, inducing voids from which crazing or shear yielding of the matrix may initiate, and (2) they also prevent craze propagation by branching. The ability of rubber to initiate craze and to prevent it from extending into crack greatly depends on the state of dispersion of rubber in PP. A comparison of run B with run a, and run A with run b indicates that elastomer particles can improve impact strength much more than fibrils can (Table IV). For run a, fibrils are fine and long ($L/D \approx 17$) with about a ninefold increase in impact strength. Fibrils are coarse and long ($L/D \approx 18$) in run A with about a fivefold increase. For run b, fibrils are coarse and short ($L/D \approx 10$) with a 10-fold increase in toughness. On the contrary, with spherical, elliptical, and rodlike dispersion in run B, a 15-fold increase in impact strength is ob-
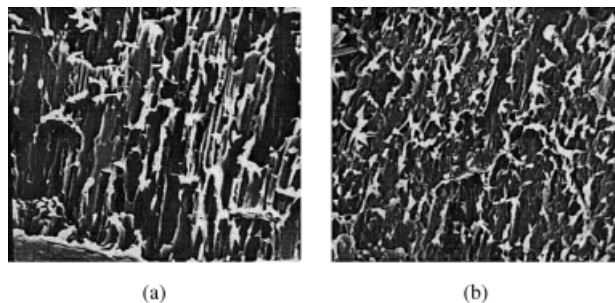
(a)   (b)

Figure 4 SEM micrographs of the A and B Izod samples cryofractured along the plane perpendicular to the fracture surface.

tained. Figure 4 presents the SEM view of the A and B Izod samples. From this figure, it can be observed that composite with long fibrils (run A) is characterized by far less matrix deformation than that of run B with spherical, elliptical, and rodlike dispersion. For fibril dispersion, the fibril ends can act as stress concentrators. The number of stress concentrators for a short fibril composite is higher than that for a long fibril composite. However, both are smaller than that with spherical elastomers. Therefore, spherical, elliptical, and rodlike elastomers in run B can initiate more voids and crazings of the matrix compared to the case of fibril elastomers in run A, which is confirmed by SEM analysis. In short, soft fibril formation suppresses the improvement of the impact strength. The coarser and longer the fibril, the worse the impact strength.

CONCLUSIONS

A study aimed at investigating soft fibril formation based on the viscosity ratio and effect of fibrillar morphology on properties of PP/EOC (75/25) blends was performed. SEM analysis showed that EOC domains become larger with the increase of viscosity ratio (T direction). Fibril formation was created along the flow direction in the case of both $\eta_d/\eta_m \approx 1$ and $\eta_d/\eta_m > 1$. Fibril formation at $\eta_d/\eta_m > 1$ indicated that the viscosity ratio is not the only factor to determine the morphology of the blends. Incorporation of EOC in PP resulted in a decrease of the tensile and flexural properties and an increase of the impact strength. EOC fibrils contribute nothing to the improvement of tensile and flexural properties because of their low strength. The increasing extent in impact strength with soft fibril morphology was lower than that with spherical, elliptical, and rodlike morphology because the number of stress concentrators in the case of fibril elastomers is less than that with spherical elastomers. The coarser and longer the fibril, the worse the impact strength.

REFERENCES

1. D'Orazio, L.; Mancarella, C.; Martuscelli, E.; et al. Polymer 1999, 40, 2745.
2. Choudhary, V.; Varma, H. S.; Varma, I. K. Polymer 1991, 32, 2534.
3. Yamaguchi, M.; Suzuki, K.; Miyata, H. J Polym Sci Part B Polym Phys 1999, 37, 701.
4. Gupta, A. K.; Purwar, S. N. J Appl Polym Sci 1984, 29, 1595.
5. Gupta, A. K.; Purwar, S. N. J Appl Polym Sci 1985, 30, 1777.
6. Kuleznev, V. N. Blends of Polymers; Khimiya: Moscow, 1980.
7. Taylor, G. I. Proc R Soc London 1934, A134, 501.
8. Tsebrenko, M. V.; Rezanova, N. M. Polym Eng Sci 1980, 20, 1023.
9. Min, K.; White, J. L. Polym Eng Sci 1984, 24, 1327.
10. Kim, B. K.; Do, I. H. J Appl Polym Sci 1996, 61, 439.
11. Baranov, A. O.; Medintsevs, T. I.; Zhorina, L. A.; et al. J Appl Polym Sci 1999, 73, 1563.
12. Danesi, S.; Porter, R. S. Polymer 1978, 19, 448.
13. Van der Wal, A.; Nijhot, R.; Gaymans, R. J. Polymer 1999, 40, 6031.
14. Dao, K. C. Polymer 1984, 25, 1527.
15. Kim, B. K.; Do, I. H. J Appl Polym Sci 1996, 60, 2207.
16. Kim, B. K.; Kim, M. S.; Kim, K. J. J Appl Polym Sci 1993, 48, 1271.
17. Cox, R. G. J Fluid Mech 1969, 37, 601.
18. Tomotika, S.; Cox, R.; Mason, S. G. J Colloid Sci 1972, 38, 395.
19. Carriere, C. J.; Silvis, H. C. J Appl Polym Sci 1997, 66, 1175.